

5. Wick, O. J. (ed.) *Plutonium Handbook: a Guide to the Technology* 33–57 (American Nuclear Society, LaGrange Park, IL, 1980).
6. Stewart, G. R. & Elliott, R. O. *Actinides in Perspective Abstracts* Lawrence Berkeley Laboratory Report no. 12441 206–207 (Lawrence Berkeley National Laboratory, Berkeley, CA, 1981).
7. Nagamatsu, J., Nakagawa, N., Muranaka, T., Zenitani, Y. & Akimitsu, J. Superconductivity at 39 K in magnesium diboride. *Nature* **410**, 63–64 (2001).
8. Werthamer, N. R., Helfand, E. & Hohenberg, P. C. Temperature and purity dependence of the superconducting critical field, H_{c2} . III. Electron spin and spin-orbit effects. *Phys. Rev.* **147**, 295–302 (1966).
9. Clogston, A. M. Upper limit for the critical field in hard superconductors. *Phys. Rev. Lett.* **9**, 266 (1962).
10. Bean, C. P. Magnetization of hard superconductors. *Phys. Rev. Lett.* **8**, 250–253 (1962).
11. Wolfer, W. G. Radiation effects in plutonium. *Los Alamos Sci.* **26**, 274–285 (2000).
12. Campbell, A. M. & Evetts, J. E. Flux vortices and transport currents in type II superconductors. *Adv. Phys.* **21**, 199–427 (1972).
13. Tokiwa, Y. *et al.* Magnetic and Fermi surface properties of UPtGa₅. *J. Phys. Soc. Jpn* **71**, 845–851 (2002).
14. Mathur, N. D. *et al.* Magnetically mediated superconductivity in heavy fermion compounds. *Nature* **394**, 39–43 (1998).

Acknowledgements We thank Z. Fisk and C. Varma for discussions. Work at Los Alamos and Florida was performed under the auspices of the US Department of Energy.

Competing interests statement The authors declare that they have no competing financial interests.

Correspondence and requests for materials should be addressed to J.L.S. (e-mail: sarrao@lanl.gov).

Electric-field-induced capillary attraction between like-charged particles at liquid interfaces

M. G. Nikolaidēs*†, A. R. Bausch*†, M. F. Hsu*, A. D. Dinsmore*†, M. P. Brenner‡, C. Gay§ & D. A. Weitz*‡

* Department of Physics; and † Division of Engineering and Applied Sciences, Harvard University, Cambridge, Massachusetts 02138, USA
 ‡ CRPP-CNRS, Avenue Schweitzer, 33600 Pessac, France

Nanometre- and micrometre-sized charged particles at aqueous interfaces are typically stabilized by a repulsive Coulomb interaction. If one of the phases forming the interface is a nonpolar substance (such as air or oil) that cannot sustain a charge, the particles will exhibit long-ranged dipolar repulsion¹; if the interface area is confined, mutual repulsion between the particles can induce ordering² and even crystallization^{3,4}. However, particle ordering has also been observed in the absence of area confinement⁵, suggesting that like-charged particles at interfaces can also experience attractive interactions⁶. Interface deformations are known to cause capillary forces that attract neighbouring particles to each other, but a satisfying explanation for the origin of such distortions remains outstanding^{7,8}. Here we present quantitative measurements of attractive interactions between colloidal particles at an oil–water interface and show that the attraction can be explained by capillary forces that arise from a distortion of the interface shape that is due to electrostatic stresses caused by the particles’ dipolar field. This explanation, which is consistent with all reports on interfacial particle ordering so far, also suggests that the attractive interactions might be controllable: by tuning the polarity of one of the interfacial fluids, it should be possible to adjust the electro-

static stresses of the system and hence the interparticle attractions.

The mismatch in dielectric constants of adjacent fluids can result in asymmetric charging of particles adsorbed at their interface; if one of the fluids is water, then the aqueous surface acquires a charge, which combines with the screening ions in the water to produce an effective dipole moment of the particle, leading to repulsion^{1,2,9}. By contrast, the origin of an attractive interaction is less well understood, even though interface deformation is known to give rise to capillary forces and a logarithmic attraction between neighbouring particles^{10–12}. For sufficiently large particles, the deformation is caused by gravity; the particle weight is balanced by surface tension, deforming the interface⁴. This results in the clumping of breakfast cereals at the surface of a bowl of milk, and has been harnessed to self-assemble millimetre-sized particles at interfaces¹³. However, the buoyancy mismatch of micrometre-sized colloidal particles is too small to deform the interface significantly and the resulting attractive energies are far smaller than thermal energy¹⁴.

An alternative candidate for the origin of the attraction is wetting of the particles, which also deforms the interface; however, a spherical particle positions itself exactly to achieve the equilibrium contact angle without distorting the interface unless the particles are constrained to a thin layer of fluid^{7,14}. Another candidate for the origin of the attraction is surface roughness, which might also deform the interface; however, the roughness required is far greater than that which typically exists on colloidal particles⁸. A final candidate for the origin of the attraction is thermal fluctuations; entropic interactions lower the free energy of the interface when two particles approach, resulting in a Casimir type of effective attraction^{15,16}. However, the resulting forces are too small to cause a significant attraction for colloid particles.

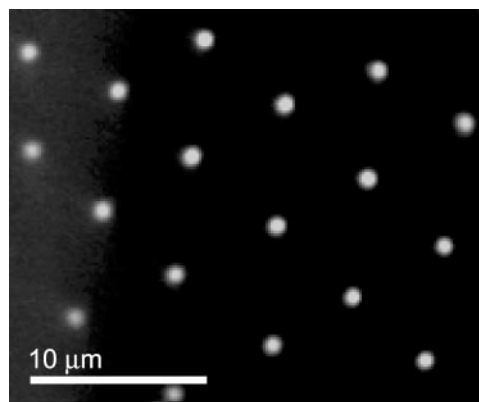


Figure 1 Interfacial colloidal particle ordering induced by repulsive interactions. The figure shows a fluorescence microscopy image of an ordered structure of colloidal particles at an oil–water interface, demonstrating the long range of the repulsive interaction. We use poly(methyl methacrylate) (PMMA) particles, sterically stabilized with poly(hydroxystearic acid)²¹. The particles have a radius of $a = 0.75 \mu\text{m}$ and are suspended in decahydronaphthalene (decalin) at a volume fraction of 0.01%. The particle cores are labelled with fluorescent dye. An emulsion of water drops in oil is produced by gently shaking around $2 \mu\text{l}$ of deionized water in 1 ml of the decalin–PMMA mixture, whereupon particles adsorb at the oil–water interface. The particles are strongly bound to the interface owing to the surface energies; this determines the contact angle. They are never observed to escape, which implies that the particles are trapped by a barrier of several tens of $k_B T$. They are observed with a charge-coupled device (CCD) camera mounted on an inverted fluorescence microscope, and the images are recorded on videotape. Sequences of interest are digitized and the particle positions are determined with particle tracking routines²². The mean squared displacement measured at short delay times provides a measure of the particle diffusion coefficient, which is intermediate between that for a particle in the water and in the oil, confirming that the particles are at the interface, partially extending into each of the fluids.

† Present address: Lehrstuhl für Biophysik - E22, Technische Universität München, Germany (M.G.N. and A.R.B.); Department of Physics, University of Massachusetts, Amherst, Massachusetts 01003-4525, USA (A.D.D.).

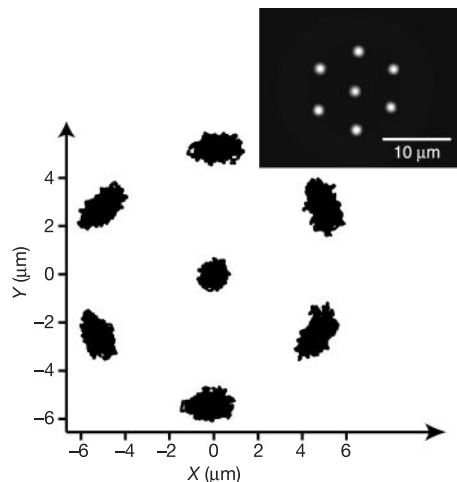


Figure 2 Scatter plot showing positions of a seven-particle hexagonal crystallite on a water droplet of 24 μm radius. The particles maintained this configuration for more than 30 min; 5 min of data, extracted at time intervals of 1/30 s are shown. The inset shows a fluorescent microscope image of the crystallite.

To investigate this question further, we quantified the attractive interaction between like-charged particles at a water–oil interface. A typical configuration of colloidal particles at the interface of a large water drop in oil is shown in Fig. 1. The long range of the repulsive interaction is apparent from the large particle separation. Moreover, this repulsion, combined with the geometric confinement resulting from the finite area of the emulsion drop, which is completely covered with particles, causes the pronounced ordering of the particles. But even when the particle coverage is not complete, ordering can still be observed, as illustrated by the inset in Fig. 2, which shows a group of seven particles in a hexagonal crystallite. These were the only particles on the surface of a large water drop, and the crystallite remained stable for more than 30 min. The persistence of this structure over long times is clear evidence of a long-ranged attractive interaction (Fig. 3).

To extract the interaction potential, we exploit the symmetry of the geometry and measure the probability distribution, $P(r)$, of the centre-to-centre distance, r , of the centre particle to each of the outer particles. To obtain the interparticle potential $V(r)$, we invert the Boltzmann distribution:

$$P(r) \propto \exp\left\{-\frac{V(r)}{k_B T}\right\} \quad (1)$$

The potential has a minimum at an interparticle separation of $r_{\text{eq}} = 5.7 \mu\text{m}$, and is well described as harmonic with a spring constant of $k = 23k_B T \mu\text{m}^{-2}$ (Fig. 3).

The motion of any given particle in the crystallite is influenced by the pair interactions with all the other particles; however, by analysing only the radial distance of the outer particles to the centre particle, these many-particle effects are largely cancelled by symmetry. This was confirmed by molecular dynamics simulation of seven particles in the same configuration, interacting with the same pair potential; an uncertainty of about 10–20% in r_{eq} and k was introduced by many-particle effects.

What is the origin of this attraction? A force, F , on the particles normal to the interface distorts the interface, leading to an interparticle capillary attraction:

$$U_{\text{interface}}(r) = \frac{F^2}{2\pi\gamma} \log\left(\frac{r}{r_0}\right) \quad (2)$$

where γ is the interfacial energy and r_0 is an arbitrary constant¹².

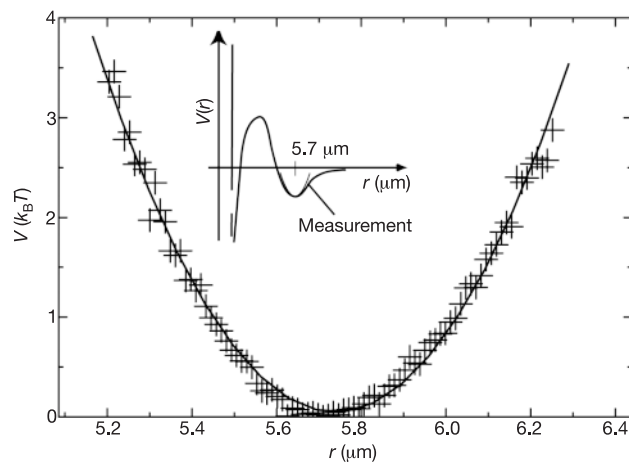


Figure 3 Secondary interparticle potential minimum derived from experimental observations. The data points are obtained from the particle distribution function of the crystallite shown in Fig. 2. The minimum at a separation of 5.7 μm produces the observed hexagonal crystallite. The inset is a sketch of the full interparticle potential and includes the repulsive barrier that stabilizes the particles, and a deep primary minimum at short range that is due to van der Waals attraction. These crystallites were observed to collapse and form a gel after several hours, confirming the presence of the primary minimum and the large repulsive barrier. The accessible range of particle separation allows us to explore the shape of the secondary minimum; the repulsive potential is sufficiently large that we cannot explore the shape or magnitude of the primary attractive well using thermal fluctuations.

Decreasing γ or increasing F increases the interfacial distortion, increasing the capillary attraction. The gravitational force of the colloidal particles on the interface is about 10^{-14} N, far too small to cause the attraction. There is, however, another natural cause for F : The dipolar fields around each particle create electrical stresses that distort the oil–water interface. The sum total of this stress is the net force F that the particle exerts on the interface.

The electrical stresses arise because oil and water have very different dielectric constants: $\epsilon_{\text{oil}} \approx 2$ and $\epsilon_{\text{water}} \approx 80$. When field lines cross the interface, the intensity of the electric field E and the electrostatic energy density $\frac{1}{2}\epsilon\epsilon_0 E^2$ are thus roughly 40 times smaller in water than in oil. Here ϵ_0 is the dielectric constant of vacuum. As a result, the free interface tends to move towards the oil to lower the energy. This is equivalent to a pressure being exerted on the interface towards the oil. The colloidal particle therefore behaves as if pulled into the water by an external force F , as shown schematically in Fig. 4. Thus the particles, which are the source of the electric fields, tend to be surrounded by water, lowering the total electrostatic energy. This effect is analogous to electrostriction¹⁷ and to electro-wetting¹⁸.

The force F can be calculated by the integral of the electric pressure $\frac{1}{2}\epsilon_0\epsilon_{\text{oil}}E_{\text{oil}}^2$ over the free surface. Because the dipolar electric field vanishes like $1/r^3$ and hence the electrostatic pressure vanishes like $1/r^6$, the effect is concentrated very close to the particle, within a distance of order the particle radius a from the contact line. Beyond that distance, the distortion is indistinguishable from any other source of interfacial distortion with the same strength F . A rough estimate of F is obtained by considering that the total electric dipole P of the particle is concentrated at the centre of the water-wetted area. The dipolar field in the oil near the interface is⁹:

$$E_{\text{oil}} \approx \frac{P}{4\pi\epsilon_{\text{oil}}\epsilon_0 r^3} \frac{2\epsilon_{\text{oil}}}{\epsilon_{\text{water}}} \quad (3)$$

The damping factor $2\epsilon_{\text{oil}}/\epsilon_{\text{water}}$ reflects the image charges required for the interface to remain an equipotential. The electric field is not

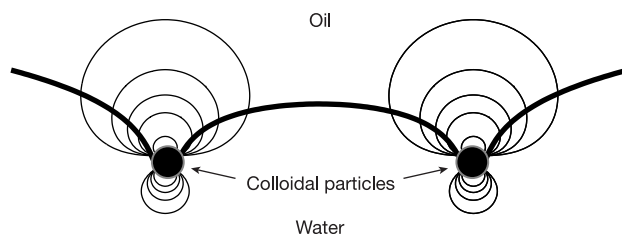


Figure 4 Sketch of the equipotential lines at the fluid interface and the resulting distortion of the oil–water interface. The distortion of the interface shape is greatly enhanced for clarity.

completely screened in the water; the screening ions are part of the charge distribution causing the dipolar fields¹. Integrating the electrostatic pressure from $r = a_w$ to $r = \infty$, where a_w is the radius of the water-wetted region of the particle, we obtain:

$$F \approx \frac{P^2}{16\pi\epsilon_0 a_w^4} \frac{\epsilon_{oil}}{\epsilon_{water}^2} \quad (4)$$

$$U = \frac{F^2}{2\pi\gamma} \log\left(\frac{r}{r_0}\right) + \frac{P^2}{4\pi\epsilon_0 r^3} \frac{2\epsilon_{oil}}{\epsilon_{water}^2} \quad (5)$$

where the first term in equation (5) is the capillary attraction and the second term is the dipolar repulsion.

From this energy we can predict both r_{eq} and the spring constant, $k = d^2U/dr^2$:

$$\frac{r_{eq}}{a_w} \approx \left(\gamma a_w^2 \frac{\epsilon_0 a_w^3}{P^2} 768\pi^2 \frac{\epsilon_{water}^2}{\epsilon_{oil}} \right)^{1/3} \quad (6)$$

$$\frac{k}{\gamma} \approx \left(\frac{1}{(\gamma a_w^2)^8} \frac{(P^2)^8}{(\epsilon_0 a_w^3)^8} \frac{3}{2^{43}\pi^{13}} \frac{\epsilon_{oil}^8}{\epsilon_{water}^{16}} \right)^{1/3} \quad (7)$$

There are two unknown materials parameters in equations (6) and (7). The first is the dipole moment, P , which depends on the screening length, κ^{-1} (taken to be $0.1 \mu\text{m}$), and the surface charge density of the spheres. The second is the radius of the wetted area, a_w , which is determined by the equilibrium contact angle θ , through $a_w = a \sin\theta$, and which depends on the surface charge density.

We obtain agreement between the predicted potential and the experimental data (see Fig. 3) if we adopt a value for a_w that corresponds to an equilibrium contact angle of 26° , and a value for P that corresponds to a total charge on the sphere of 2×10^5 unit charges, or a density σ of 0.6 unit charges per nm^2 . Both of these values are physically reasonable. The fit corresponds to $r_{eq} = 5.7 \mu\text{m}$ and $k \approx 23k_B T \mu\text{m}^{-2}$, both in good agreement with the experimentally measured values. The interfacial distortion predicted by the theory is given by the estimate $h \approx F/(2\pi\gamma) \log(r_{eq}/a)$, and is $h \approx 10 \text{ nm}$, too small to be observed with an optical microscope.

Both the repulsive and the attractive components of the interaction potential depend strongly on the dipole moment, $P = (\sigma/\kappa)\pi a_w^2$. This is directly proportional to the zeta potential of the particle surface, which in turn sensitively depends on surface charge, surface chemistry, and the screening length, κ^{-1} , set by the ion concentration in the water¹⁹. Thus, for example, if the surface charge remains constant, small changes in κ^{-1} change P a great deal, whereas if the surface charge varies and the zeta potential remains constant, there will be no variation of P with κ^{-1} . The attractive interaction is sensitively dependent on P ; thus, if the surface charge remains constant, the attraction becomes negligible compared to $k_B T$ even for low concentrations of added salt, as shown in the Supplementary Information. To verify the sensitivity of the attraction on P , the measurements were repeated with 5 mM NaCl added

to the water; only the repulsive interaction remained and its range was reduced, leading to a correspondingly lower particle stability, as shown in the Supplementary Information. These results also confirm that the particles are charged on the aqueous side, rather than the oil side²⁰. More generally, the existence of a measurable attractive interaction depends on both P and a_w , and thus is sensitive to surface properties, charge and pH, as well as salt concentration.

Although our theory does not fully account for the geometry of the wetted region, it nevertheless captures the essential physics: Dipolar electric fields induce surface charges that distort the interface; the dipolar interaction causes repulsion, while the interfacial distortion causes capillary attraction. This behaviour has broader implications for interfacial and colloid chemistry, because adsorption of charged particles at fluid interfaces is a common phenomenon in foods, drugs, oil recovery, and even biology. □

Received 18 April; accepted 10 September 2002; doi:10.1038/nature01113.

- Pieranski, P. Two-dimensional interfacial colloidal crystals. *Phys. Rev. Lett.* **45**, 569–572 (1980).
- Onada, G. Y. Direct observation of two-dimensional, dynamical clustering and ordering with colloids. *Phys. Rev. Lett.* **55**, 226–229 (1985).
- Denkov, N. D., Velev, O. D., Kralchevsky, P. A. & Ivanov, I. B. Two-dimensional crystallization. *Nature* **361**, 26 (1993).
- Wickmann, H. H. & Korley, J. N. Colloid crystal self-organization and dynamics at the air/water interface. *Nature* **393**, 445–447 (1998).
- Ruiz-García, J., Gámez-Corralles, R. & Ivlev, B. I. Formation of two-dimensional colloidal voids, soap froths, and clusters. *Phys. Rev. E* **58**, 660–663 (1998).
- Quesada-Pérez, M., Moncho-Jordá, A., Martínez-López, F. & Hidalgo-Álvarez, R. Probing interaction forces in colloidal monolayers: Inversion of structural data. *J. Chem. Phys.* **115**, 10897–10902 (2001).
- Kralchevsky, P. A. & Denkov, N. D. Capillary forces and structuring in layers of colloid particles. *Curr. Opin. Colloid Interf. Sci.* **6**, 383–401 (2001).
- Stamou, D., Duschl, C. & Johannsmann, D. Long-range attraction between colloidal spheres at the air-water interface: The consequence of an irregular meniscus. *Phys. Rev. E* **62**, 5263–5272 (2000).
- Hurd, A. J. The electrostatic interaction between interfacial colloidal particles. *J. Phys. A* **18**, L1055–L1060 (1985).
- Chan, D. Y. C., Henry, J. D. & White, L. R. The interaction of colloidal particles collected at fluid interfaces. *J. Colloid Interf. Sci.* **79**, 410–418 (1981).
- Kralchevsky, P. A., Paunov, V. N., Ivanov, I. B. & Nagayama, K. Capillary meniscus interaction between colloidal particles attached to a liquid–fluid interface. *J. Colloid Interf. Sci.* **151**, 79–94 (1992).
- Morse, D. C. & Witten, T. A. Droplet elasticity in weakly compressed emulsions. *Europhys. Lett.* **22**, 549–555 (1993).
- Bowden, N., Terfort, A., Carbeck, J. & Whitesides, G. M. Self-assembly of mesoscale objects into ordered two-dimensional arrays. *Science* **276**, 233–235 (1997).
- Kralchevsky, P. A. & Nagayama, K. Capillary interactions between particles bound to interfaces, liquid films and biomembranes. *Adv. Colloid Interf. Sci.* **85**, 145–192 (2000).
- Goulian, M., Bruinsma, R. & Pincus, P. Long-range forces in heterogeneous fluid membranes. *Europhys. Lett.* **22**, 145–150 (1993).
- Golestanian, R., Goulian, M. & Kardar, M. Fluctuation-induced interactions between rods on a membrane. *Phys. Rev. E* **54**, 6725–6734 (1996).
- Landau, L. D. & Lifshitz, E. M. *Electrodynamics of Continuous Media* (Addison Wesley Publishing, Pergamon Press, Reading, MA, 1964).
- Berge, B. Electrocapillarity and wetting of insulator films by water. *C. R. Acad. Sci. II* **317**, 2, 157–163 (1993).
- Russel, W. B., Saville, D. A. & Schowalter, W. *Colloidal Dispersions* (Cambridge Univ. Press, Cambridge, UK, 1989).
- Aveyard, R. *et al.* Measurement of long-range repulsive forces between charged particles at an oil-water interface. *Phys. Rev. Lett.* **88**, 246102–1–4 (2002).
- Pusey, P. N. & van Meegen, W. Phase-behaviour of concentrated suspensions of nearly hard colloidal spheres. *Nature* **320**, 340–342 (1986).
- Crocker, J. C. & Grier, D. G. Methods of digital microscopy for colloidal studies. *J. Colloid Interf. Sci.* **179**, 298–310 (1996).

Supplementary Information accompanies the paper on Nature's website (<http://www.nature.com/nature>).

Acknowledgements We thank B. Berge and T. M. Squires for discussions. We gratefully acknowledge support from the NSF, the Materials Research Science and Engineering Center through the auspices of the NSF and the Division of Mathematical Sciences. A.B. acknowledges the support from the Emmy Noether-Program of the DFG.

Competing interests statement The authors declare that they have no competing financial interests.

Correspondence and requests for materials should be sent to D.A.W. (e-mail: weitz@deas.harvard.edu).